

# Strategic Synthesis of 2D and 3D Conducting Polymers and Derived Nanocomposites

Munziya Abutalip, Guldana Zhigerbayeva, Dana Kanzhigitova, Perizat Askar, Yelriza Yeszhan, Tri Thanh Pham, Salimgerey Adilov,\* Rafael Luque,\* and Nurxat Nuraje\*

In recent decades, there has been a great deal of interest in conducting polymers due to their broad applications. At the same time, various synthetic techniques have been developed to produce various nanostructures of the conducting polymers with their fascinating properties. However, the techniques for the manufacture of 2D nanosheets are either complex or expensive. No comprehensive approach for constructing 2D and 3D materials or their composites has been documented. Herein, a simple and scalable synthetic protocol is reported for the design of 2D, 3D, and related conducting polymer nanocomposites by interface manipulation in a bicontinuous microemulsion system. In this method, diverse bicontinuous thin layers of oil and water are employed to produce 2D nanosheets of conducting polymers. For the fabrication of 3D polypyrrole (PPY) and their composites, specially designed linkers of the monomers are applied to lock the 3D networks of the conducting polymers and their composites. The technique can be extended to the fabrication of most conducting polymer composites, being cost-effective and easily scalable. The optimum electrical conductivity obtained for 2D PPY nanosheets is  $219 \text{ S cm}^{-1}$ , the highest literature value reported to date to the best of knowledge.

## 1. Introduction

Organic conjugated polymers have shown applications in the field of light-emitting diode (LED),<sup>[1]</sup> thin-film transistors,<sup>[2]</sup> solar cells,<sup>[3]</sup> batteries,<sup>[4]</sup> and supercapacitors<sup>[5]</sup> and so on. Various nanostructures possess unique electrical, mechanical, and optical properties. For example, graphene, 2D materials, possesses high electron mobility and high stiffness.<sup>[6]</sup> With the discovery of conducting polymers, recent research<sup>[7]</sup> revealed that the dimensionality of conducting polymer nanostructures is a critical parameter to tune its unique electrical properties. Fabrication of nanostructured conducting polymers mainly includes two different templated syntheses including hard<sup>[8,9]</sup> and soft templating approaches.<sup>[10,11]</sup> Furthermore, various polyaniline (PANI) structures including nanoparticles,<sup>[12,13]</sup>

M. Abutalip, G. Zhigerbayeva, D. Kanzhigitova, P. Askar, Y. Yeszhan, N. Nuraje

Department of Chemical & Materials Engineering  
School of Engineering & Digital Science  
Nazarbayev University  
Astana 010000, Kazakhstan  
E-mail: nurxat.nuraje@nu.edu.kz

M. Abutalip, N. Nuraje  
Lab of Renewable Energy Systems & Materials Science  
National Laboratory Astana  
Nazarbayev University  
Astana 010000, Kazakhstan

D. Kanzhigitova  
Department of Chemistry and Chemical Technology  
Al-Farabi Kazakh National University  
Almaty 050040, Kazakhstan


T. T. Pham

Department of Biology  
School of Sciences and Humanities  
Nazarbayev University  
Astana 010000, Kazakhstan

S. Adilov  
Department of Chemistry  
School of Sciences and Humanities  
Nazarbayev University  
Astana 010000, Kazakhstan  
E-mail: sadilov@nu.edu.kz

R. Luque  
Departamento de Química Orgánica  
Universidad de Córdoba  
Campus de Rabanales  
Edificio Marie Curie (C-3)  
Ctra Nnal IV-A, Km 396, Cordoba E14014, Spain  
E-mail: q62alsor@uco.es

R. Luque  
Peoples Friendship University of Russia (RUDN University)  
6 Miklukho Maklaya str., Moscow 117198, Russian Federation

 The ORCID identification number(s) for the author(s) of this article can be found under <https://doi.org/10.1002/adma.202208864>.

© 2022 The Authors. Advanced Materials published by Wiley-VCH GmbH. This is an open access article under the terms of the Creative Commons Attribution-NonCommercial License, which permits use, distribution and reproduction in any medium, provided the original work is properly cited and is not used for commercial purposes.

DOI: 10.1002/adma.202208864

nanoneedles,<sup>[14,15]</sup> nanotubes,<sup>[16–18]</sup> nanofibers,<sup>[19–23]</sup> nanowires,<sup>[24–26]</sup> nanosheets,<sup>[27,28]</sup> and networks,<sup>[1,29,30]</sup> have been successfully prepared, which stimulated investigations of structure–property relationships of PANI.

Such studies emphasized the importance of developing 2D morphologies to obtain superior electrical properties, especially in the desired directions, targeting high-density integrated electronic devices.<sup>[7,31–33]</sup> Conducting polymer scientists aim to design well-tailored chemical–physical characteristics of conducting polymers and fabricate their specific nanostructures for emerging technologies. Although high-cost and sophisticated techniques including electron beam evaporation, vapor–liquid–solid growth, etc., toward fabrication of 2D sheets have been developed, no general strategy has been reported to date for the design of 2D and 3D or their composites. What’s more, in the templated synthesis approach, the removal of the graphene (GO) is also an additional shortcoming to produce uniform PANI sheets. At present, 2D nanosheets of PANI produced by using ice as a hard template claimed the highest electrical conductivity of  $35 \text{ S cm}^{-1}$ , a significant improvement from previous values reported over past decades.<sup>[34]</sup>

Herein, an unprecedented, facile, and scalable synthetic strategy is reported for the design of 2D, 3D as well as nanocomposite-derived nanomaterials different from interfacial polymerization applied in liquid–liquid and other interfacial polymerization techniques.<sup>[14]</sup> In this approach, various

bicontinuous thin layers of oil and water formed nanoconfined reactors for the design of 2D nanosheets of conducting polymers zipping via interfacial polymerization (**Figure 1**). Four different reactors including pure, nonionic, cationic, and anionic interfaces were designated to tailor the morphology and properties of conducting polymer nanosheets. The ratio between oxidant and monomer is a critical parameter to control the morphology. To produce 3D conducting polymers, special linkers of conducting polymers were designed to zip/connect the conducting polymer networks. The length of the linkers is another critical parameter to control the electrical and mechanical properties of the conducting polymer networks. To generate multifunctional conducting polymer composites, the target materials were premixed with monomers to subsequently undergo interfacial polymerization to zip 3D networks with the monomer linkers. To implement the general strategy, polypyrrole was selected as conducting polymer. The optimum electrical properties obtained for the designed 2D PPY nanosheets were  $219 \text{ S cm}^{-1}$ , the highest literature-reported conductivity to date for such advanced materials.

## 2. Results and Discussion

Designing special bicontinuous reactor systems was the primary strategy to synthesize 2D, 3D conducting polymers

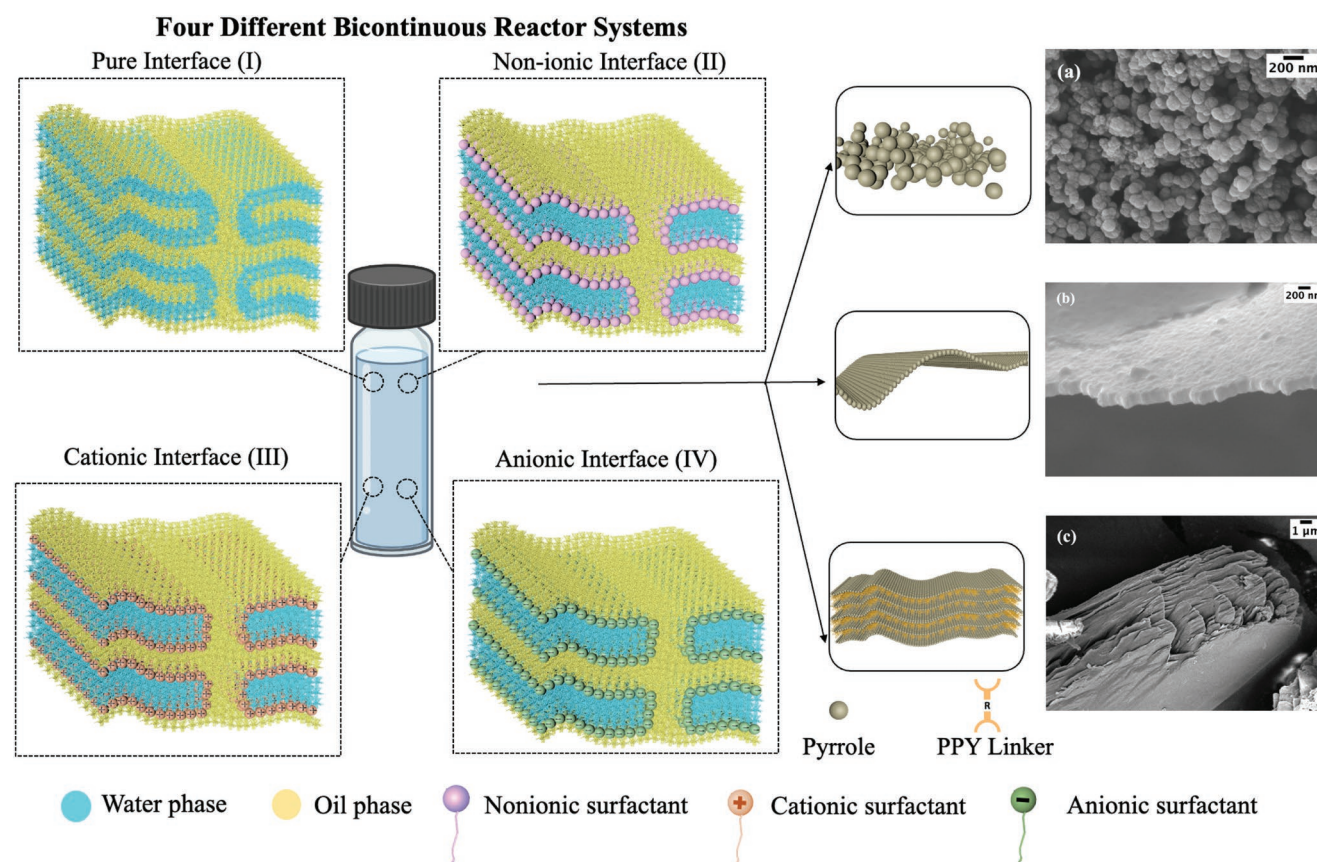


**Figure 1.** Conceptual schematic illustration of the fabrication of conductive polymers: a) particle. b) 2D and c) 3D conducting polymers and their composites using bicontinuous reactor systems.

and their composites (Figure 1). Thin layered interfaces in the bicontinuous reactor system are the main platform to control both morphology and properties of the conducting polymer materials including electrical, mechanical, and structural. Key parameters for tuning conducting polymer nanostructures include the ratio of monomer and oxidant, interface thickness and charge regularity, nature of oxidant, and doping element. Furthermore, monomer, linker, and oxidant ratios were found to be critical elements to control the morphology of conducting polymer 3D nanostructures. In all syntheses, interfacial polymerization is the main zipping tool to connect monomers and generate 2D and 3D conducting polymers.

As shown in Figure 1a, the relatively low ratio of monomer to oxidant (7/10 wt%) is one of the relevant parameters utilized to generate PPY nanopowder structures via interface manipulation in the non-ionic,<sup>[35]</sup> pure,<sup>[36,37]</sup> cationic and anionic<sup>[38]</sup> interfaces bicontinuous reactors designed from the phase diagram (Figures S1 and S6, Supporting Information). A high monomer-to-oxidant ratio can be controlled to produce 2D-PPY nanosheets (1.2/1 wt%) (Figure 1b). In the fabrication of 3D PPY and nanocomposites (Figure 1c), pyrrole special linkers (Scheme S1, Supporting Information) were designed to react with pyrrole monomers in the bicontinuous reactors to generate layered PPY nanostructures.

In the synthesis of nanostructures of conducting polymers (PPY), the interface is a major driving force to manipulate the formation of conducting polymer nanostructures. For this investigation, four different interfaces (Figure 1I,II,III,IV), such as pure oil/water interface (Figure 1I), non-ionic interface (Figure 1II), cationic interface (Figure 1III), and anionic interface (Figure 1IV), were selected to study PPY nanostructure

formation. The role of the surfactant in the bicontinuous thin-layered system is to produce a uniform interfacial differentiation between water and oil layers. Except for the negatively charged interface, the other three interfaces including cationic (Figure 1III), non-ionic (Figure 1II), and pure water/oil interfaces (Figure 1I), were able to produce 2D nanosheets of PPY under optimum conditions. This can be controlled by modifying the reactor composition, where the oil-to-water ratio plays a crucial role. The thickness of these layers depends on the amount of oil and water in the system. Non-ionic bicontinuous reactor (NBCR) consisting of water layers and oil layers aligned with the nonionic interface (Figure 1II) was selected to investigate the effect of monomer/oxidant ratio on the formation of PPY nanostructures.

PPY materials exhibited a variety of structural changes due to the oil-to-water ratio effect. The optimum ratio of all components including oil ratio (from 50 to 80 wt%), water content (from 5 to 20 wt%), and surfactant concentration (Figure 2), changed correspondingly to 100 wt% of the NBCR system, are key parameters in the design of uniform free-standing nanosheets (Figure 2b). Experimentally, the excess or deficiency of the monomer in the matrix leads to the formation of structural defects or nanopowders (Figure 2a,c). Although other temperature ranges were explored, the room temperature was found to be the optimum polymerization temperature to generate 2D nanosheets.

2D-PPY nanosheets were formed via the assembly of nanobeads of PPY. At low oxidant quantities (FeCl<sub>3</sub>, 5 to 20 wt% of water) (Figure S3, Supporting Information), PPY polymer chains have a chance to grow in the bidimensional direction since the nucleation sites are relatively low and the growth process of PPY is dominant over the nucleation process.

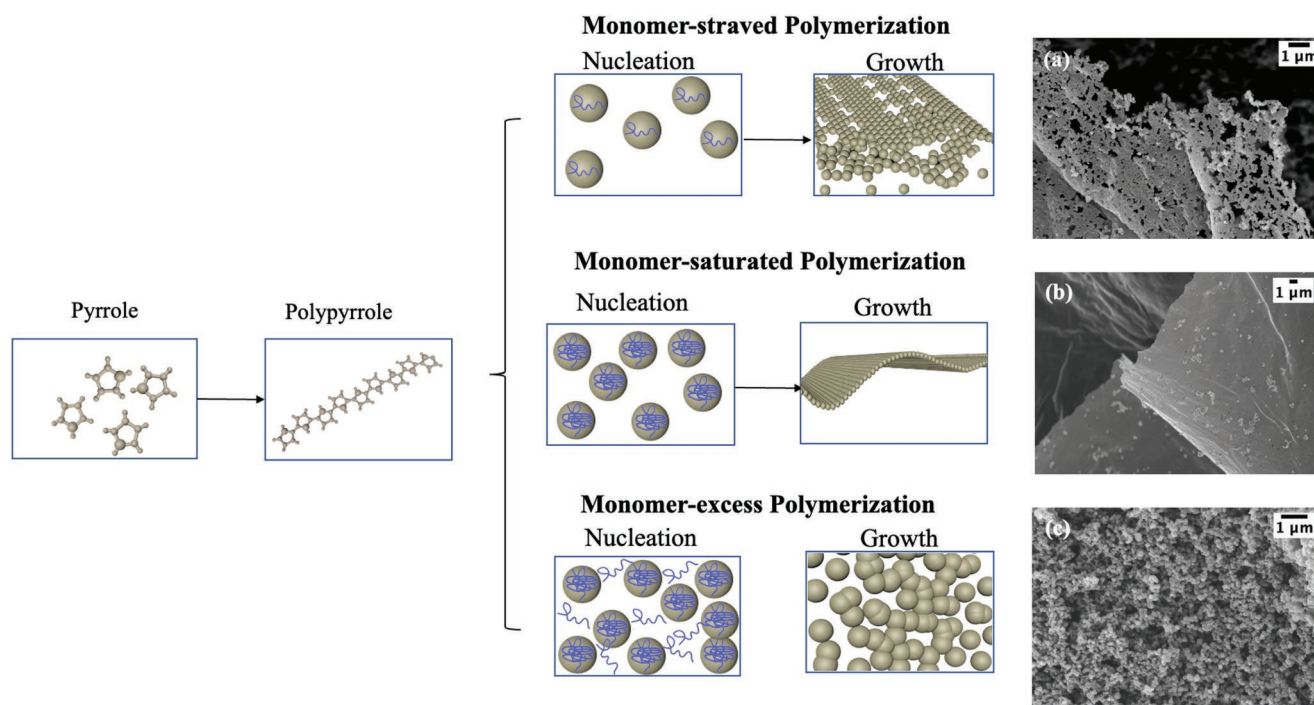


**Figure 2.** The effect of the monomer to oxidant ratio on the formation of 2D nanostructure of PPY, a) not-complete 2D nanosheet, b) complete 2D nanosheet, and c) particle-networks.

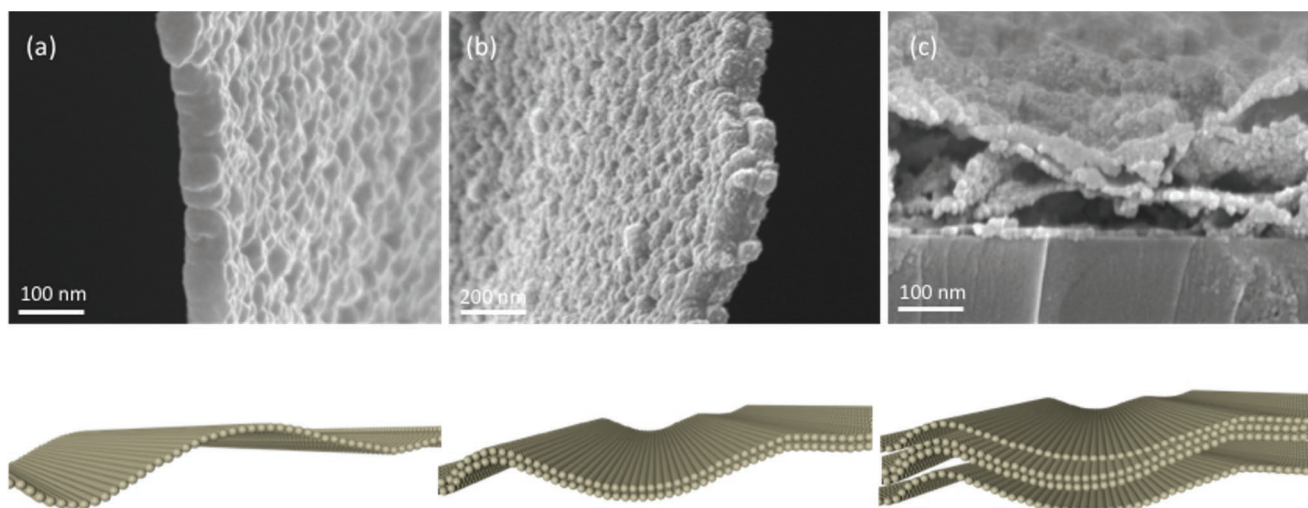


**Figure 3.** The layered structure of PPY conducting nanosheets at different oil/water/surfactant ratios. SEM images and molecular models of non-ionic interface reactors: a) Reactor 60/10/30, b) Reactor 60/15/25, and c) Reactor 40/30/30.

In the case of the low monomer ratio, the high amounts of oxidants created more nucleation sites, which can be a dominant step relative to the growth process. Thus, nanopowder formation of PPY was found to be favored at low monomer ratios (Figure 2c), not the growth of the 2D nanosheets.

The average thickness of such films was found to be 25–150 nm. Since the nonionic interface does not carry any charges and does not interact with monomers or oligomer chains, its influence on the polymerization process is minimum. It acts as a barrier that does not allow penetration of the monomer chains to other regions and controls particle distribution on the interface. Polymer chains, therefore, grow in 2D directions and form a well-distributed film on the interface. The above findings are also confirmed by the addition of another oxidant (Ammonium persulfate, APS) (Figure S4, Supporting Information) in the NBCR.

An appropriate manipulation of the interface is critical to build monolayered, double-layered, and even multi-layered 2D free-standing nanosheets. Due to the wrinkle and wavy structural nature of the single layer, the formation of multilayered sheets including 2D conducting polymers is not perfectly packed. **Figure 3** shows the effect of water content on the formation of nanosheets synthesized under the nonionic interface (**Figure 4a**) as the water content gradually increases from 10 to 30 wt%. As the amount of both water and surfactant in the NBCR exceeds 30%, many-layered polymer sheets were found, where monomer concentrations were relatively reduced,

a major parameter in the formation of multilayered film structures. The water-to-surfactant ratio is a key parameter to achieve the layered structure of the film (packed layers increased with an increase in water content in the nanoreactor system).

In both cationic and pure oil/water interface, the density of PPY nanosheets by the bicontinuous thin layered reactor in the absence of surfactant is relatively high (while 2D nanosheets of PPY were still found) due to no molecular barrier formation at the interface (**Figure 4b**) (Table S1, Supporting Information). This allows PPY chains to diffuse through interfaces and form thicker and denser structured films (**Figure S7**, Supporting Information). The average thickness of such type of nanosheet was found to be 195–650 nm. 2D films can be easily formed in the cationic or positively charged interface system (**Figure 4c**), because of the repulsion between positively charged interface and PPY chains and the preference for growth among PPY polymer chains. Although 2D PPY nanosheets are still formed, the positive charge of the interface repulses pyrrole particles and leads instead to porous 2D nanosheet formation.

The presence of the counter ions at the interface (anionic bicontinuous reactor system) does not allow the 2D growth of the polymer nanosheets, because they have a strong electrostatic attraction with polymer chains (**Figure 4d**). The average thickness of the synthesized materials is in a range between 25 and 220  $\mu\text{m}$ .

Conjugated polymers become more conductive with the addition of doping agents. In our designed reactor systems,

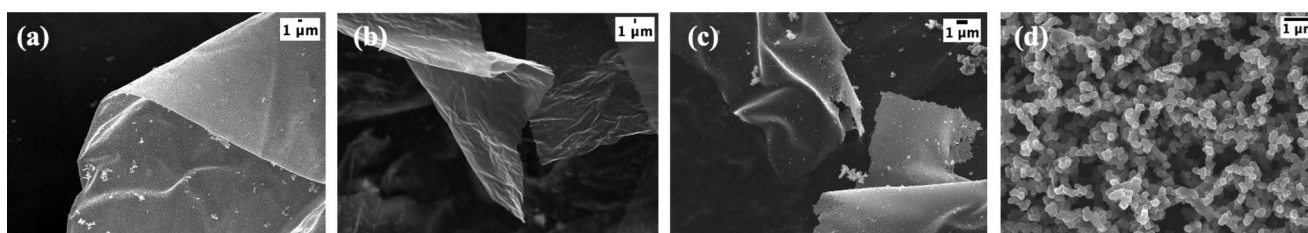


**Figure 4.** a) PPY nanosheets fabricated by a non-ionic bicontinuous reactor. b) PPY nanosheets by pure oil/water interface. c) Cationic bicontinuous reactor. d) 3D bead connected networks PPY by the anionic bicontinuous reactor.

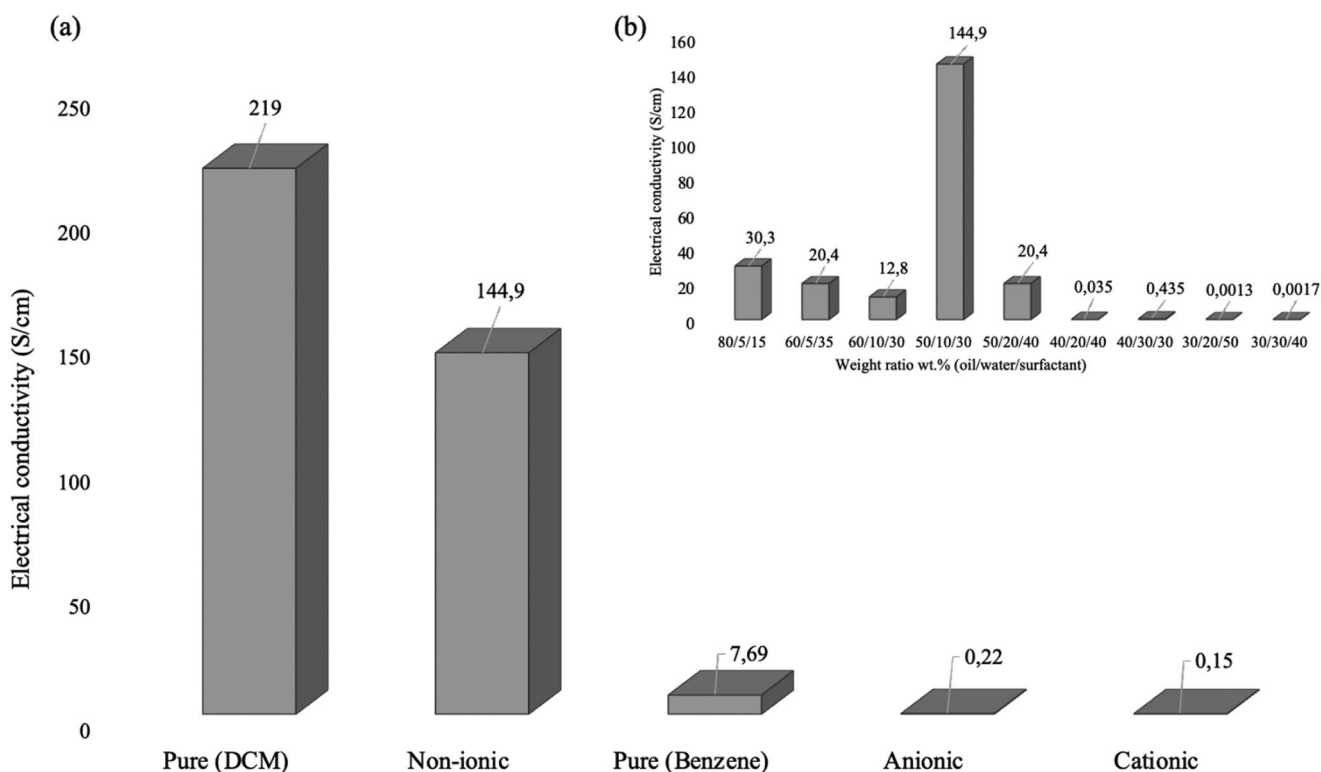


**Figure 5.** a,b) Electrical conductivity of all interfaces (a) and b) non-ionic interface (b) reactors with variable oil-to-water ratios.

polymerization of pyrrole monomer occurs in the presence of ferric chloride and hydrochloric acid as doping agents. The thickness of 2D polypyrrole nanosheets varies from 25 to 400 nm due to the factors mentioned above in the morphological studies. These parameters significantly influenced the electrical properties of 2D PPY films as shown in **Figure 5**, and more detailed information can be found in Tables S2 and S3 (Supporting Information). Table S3 (Supporting Information) reports the average conductivity values obtained from four different reactors.

The special design of our reactors with four different interfaces allows the control of the electrical properties of synthesized materials. The highest conductivity,  $219 \text{ S cm}^{-1}$ , was obtained for the nanosheet fabricated by the pure interface reactor system (DCM system) due to the absence of an interfacial barrier and easy transportation of doping agents to the polymer matrix. The second highest conductivity,  $144.9 \text{ S cm}^{-1}$ , was obtained by a non-ionic interface at the optimal ratio of oil to water (50/10 wt%) since it does not interfere with the transportation of doping molecules. In addition, the ratio between monomer and oxidant is another important parameter that affects the electrical properties of 2D conducting polymers due to the uniformity and relatively low thickness. The electrical conductivity range depends on the uniformity of the 2D conducting polymers. In the case of cationic and anionic interfaces, the morphology of the synthesized materials was more porous and not uniform, which increased the distance between particles and resulted in lower conductivity (**Figure 5**). The conductivity of 2D PPY nanosheets obtained by pure and neutral interfaces is ten times higher than the data reported

so far for 2D conducting polymers.<sup>[32]</sup> Controlling the interface and doping, the electrical properties of conducting polymers could be effectively fine-tuned.

To design 3D PPY conducting polymer networks, special linkers<sup>[39]</sup> were designed (Scheme S1, Supporting Information) and mixed with the pyrrole monomer, followed by interfacial polymerization to polymerize both monomer and linker together through the interface of oil and water thin layers in a bicontinuous system. Both monomers and linkers were mixed in the oil-thin bicontinuous layers and polymerized by the introduction of oxidants. In the oxidative polymerization of pyrrole monomers and linkers, pyrrole monomers could be oxidized to form monomer radicals followed by reacting with the linkers due to their low reactivity. The ratio between the monomer and its linker is important to achieve various thickness layers and structures (**Figure 1c** and **Figure 6**). The presence of the linker in the system has a packing effect on the structure of the synthesized PPY 3D materials. At increasing linker concentrations in the reactor (as shown in **Figure 6b–d**), these layered structures tend to be packed and interconnected to form dense plate-like structures.

Furthermore, the ratio of monomer to linker from 0.5 to 4 wt% enhances the formation of layered plate-like structures (**Figure 6**; **Figure S9**, Supporting Information). The above morphology changes of 3D PPY materials were confirmed by both different linkers, which are C6 and C10 lengths (more details in Table S4, Supporting Information). Furthermore, both linkers gave the same structures as layered plates. The formation of the 3D layered structures was ascribed to the presence of bicontinuous layered structures in the reactor systems (**Figure 1I,II,III,IV** and c).

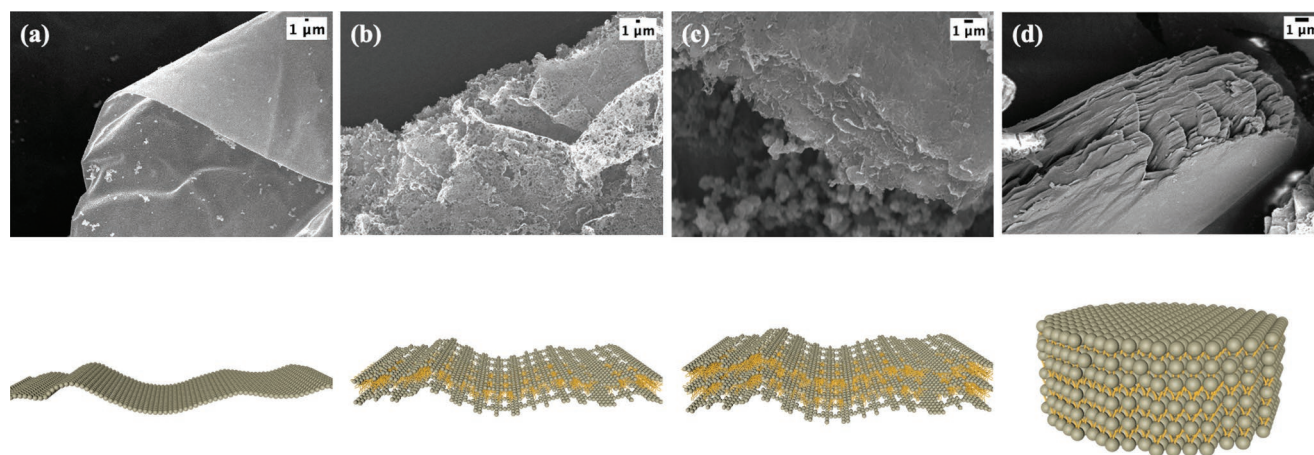


**Figure 6.** a) SEM images and illustration of 2D PPY pure nanosheet, and b–d) monomer to linker ratio effect of 3D PPY material with the linker carbon chains lengths 6. Linker concentration is increased from 0.5 wt% to 1 and 4 wt%.

Polymerization of the monomer with the linker was confirmed via FTIR studies. Figure S8 (Supporting Information) depicts FTIR spectra of 2D PPY, pure linker, and 3D PPY. Polypyrrole gives characteristic peaks for C=C double bond at  $1500\text{ cm}^{-1}$  and C–H vinyl stretching at  $\approx 3000\text{ cm}^{-1}$ .<sup>[40]</sup> Other signals corresponding to the linker become visible after the linker is polymerized with pyrrole. Namely, carbonyl stretching at  $\approx 1700$  and  $\approx 3000\text{ cm}^{-1}$  corresponding to  $\text{sp}^3$  C–H starts appearing as the amount of linkers were increased.

This strategy could be further extended to produce conducting polymer nanocomposite materials by a one-step fabrication technique of free-standing conducting polymer nanocomposites, combining the functionalities of conducting polymers and nanoparticles to create an integrated system. Such an approach was employed in the design of PPY and fluorescent carbon dots (CDs) nanocomposites. Carbon dots nanomaterials were selected as dispersed phase materials to add into the oil phase with monomers and linkers together. Carbon dots are semiconductors and have unique photoluminescence emission which makes them excellent material for medical diagnosis,<sup>[41,42]</sup> bio-imaging,<sup>[43]</sup> fluorescent sensing,<sup>[44]</sup> light emitting diodes<sup>[45]</sup> and photovoltaic devices.<sup>[46]</sup> Moreover, CDs show promising results in sensing and detecting heavy metals.<sup>[47]</sup> The best emission quenching effect has been shown by detecting iron due to the oxidation-reduction reaction of  $\text{Fe}^{2+}/\text{Fe}^{3+}$  ions. At present, the main limitation of the carbon dots is their fluorescence self-quenching effect in the dry state due to the agglomeration of the particles, which reduces light emission time.

Synthesized PPY@CD nanocomposites following the proposed methodology (premixing them with monomers and linkers) remarkably improved the brightness and photoluminescence emission of CDs (Figure S10, Supporting Information). The intensity of PPY nanocomposites increased with the addition of CDs relative to 2D PPY@CD composites and pure CD particles due to the stabilization and dispersion of CDs in the PPY matrix. The synthesized PPY@CDs nanocomposites show outstanding  $\text{Fe}^{3+}$ -ion detection capability and stability by quenching and reactivating CD nanoparticles embedded in the structure of the polymer nanosheets. The intensity of PPY nanocomposites increased with the addition

of the CDs due to the stabilization and dispersion of CDs in the PPY matrix (Figure S11, Supporting Information). Since  $\text{Fe}^{3+}$  ions have a quenching effect on CDs, the sensitivity of the polymer nanosheets was dramatically reduced by the addition of a ferric chloride solution (Figure S12, Supporting Information; **Figure 7** (middle)). PPY@CD nanocomposites could be reactivated by adding ascorbic acid, with photoluminescence returning to the initial value (Figure S12, Supporting Information; **Figure 7** (right)).

The quenching and reactivation of the PPY@CD nanocomposites proved that the proposed simple, efficient, and straightforward methodology can be utilized to design nanocomposites of conducting polymers and advanced functional materials.

### 3. Conclusion

A general, simple and scalable synthetic strategy has been developed for the design 2D and 3D, conducting polymers and their nanocomposites for the first time. This fabrication technique was established based on the four different interface bicontinuous reactors including pure, nonionic, cationic, and anionic interfaces. The nature of the interfaces, the thickness of the thin layered interfaces, the ratio monomer/oxidant ratios (and that between monomers, linkers, and oxidants) as well as doping level were found to be key parameters to control morphologies and electrical properties of the conducting polymer materials. The pure interface in the absence of the molecular layer offers relatively thicker 2D nanosheets compared to other interfaces such as cationic, nonionic, and anionic. The conductivity obtained for 2D nanosheets designed by pure interface bicontinuous systems was the highest among the four different systems, remarkably superior to literature-reported values for 2D-sheet conducting polymers.<sup>[32]</sup> 3D PPY materials were designed and successfully fabricated in the bicontinuous reactor system with inclusion of special linkers. In the synthesis of the nanocomposite, functional dispersed phase materials were added into the mixture of monomers and linkers. The proposed approach has the potential to pave the

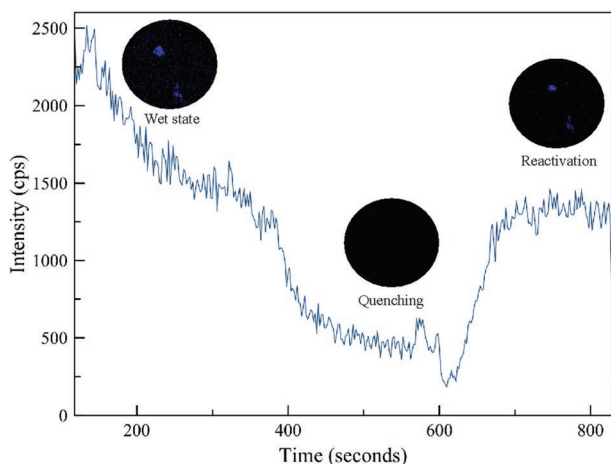


**Figure 7.** Fluorescence quenching and reactivation analysis of CDs in the PPY nanocomposite materials by confocal microscopy.

way to the design of advanced conducting polymers and their 2D-, 3D-, and nanocomposites, with promising prospects for scale-up production.

#### 4. Experimental Section

**Synthesis of 2D PPY:** The bicontinuous microemulsion polymerization method was used for the polymerization of pyrrole. In the typical experimental setup, pyrrole monomer was freshly distilled under reduced pressure before use, and deionized water (DI) was utilized as an aqueous component of the microemulsion system and an oxidant solvent for the polymerization reaction. The ferric chloride ( $\text{FeCl}_3$ ) (concentration was from 2 to 20  $\text{mg mL}^{-1}$ ) or ammonium persulfate (APS) (concentration was from 1 to 15  $\text{mg mL}^{-1}$ ) was dissolved in DI water as oxidant and hydrochloric acid (HCl) as a doping agent was introduced to control the acidity of the water fraction from pH 1 to 2. A surfactant solution of TX-100/butanol with a mass ratio of 1:1 was prepared; monomers dissolved in cyclohexane (80:20 wt%). Then, the three components were mixed to form a bicontinuous phase (Figure S2, Supporting Information) and left for 8–24 h to complete the polymerization reaction at room temperature. The formed black films and powders of the polypyrrole were washed with acetone till the non-reacted oil residue was completely removed. Synthesized PPY with  $\text{FeCl}_3$  and APS at different concentrations is shown in Figures S3 and S4 (Supporting Information).

**Synthesis of 3D PPY:** For the synthesis of 3D polypyrrole in a non-ionic reactor system, the oil/water ratio and the amount of linker based on monomer concentration were calculated. The linker was premixed with pyrrole. The ferric chloride solution ( $5 \text{ mg mL}^{-1}$ ) was selected as a catalyst. After mixing all the components, the reactor was left for 1 day. After polymerization was completed, the polypyrrole was washed using acetone and methanol. The synthesis protocol is shown in Table S4 (Supporting Information).

**Synthesis of PPY Nanocomposite:** The bicontinuous benzene/ethanol/water reactor system was employed to create the PPY nanocomposite. In a typical preparation of benzene/ethanol/water surfactant-free bicontinuous phase, the following composition was used; 1% benzene, 30% EtOH, and 69% water. All monomers and linkers were prepared in benzene; and oxidant and carbon dots were in the aqueous phase. The oxidant-to-S-CD ratio was 1:100. The components were then mixed with care to form a bicontinuous phase, which was allowed to polymerize for 8–12 h at room temperature. The obtained black solid was washed with ethanol and acetone, respectively. The obtained 2D and 3D materials were further characterized by analytical tools such as AFM, SEM, TEM, and FT-IR.

#### Supporting Information

Supporting Information is available from the Wiley Online Library or from the author.

#### Acknowledgements

M.A. and G.Z. contributed equally to this work. This work was supported by the Ministry of Education and Science of the Republic of Kazakhstan under project No. AP09258910 “Multifunctional Desulfurization Polymer Nanocomposites”, Faculty Development Competitive Research Grant of Nazarbayev University (Project ref. no. 021220FD4551) “Crosslinked 3D Nanoporous Conducting Polymer Materials via Bicontinuous Microemulsion-based Approach”. This publication was supported by RUDN University Strategic Academic Leadership Program (R. Luque).

#### Conflict of Interest

The authors declare no conflict of interest.

#### Data Availability Statement

The data that support the findings of this study are available from the corresponding author upon reasonable request.

#### Keywords

conducting polymers, electronic properties, polyaniline

Received: September 26, 2022

Revised: November 4, 2022

Published online: December 8, 2022

- [1] Y. Yang, E. Westerweele, C. Zhang, P. Smith, A. J. Heeger, *J. Appl. Phys.* **1995**, *77*, 694.
- [2] H. Klauk, *Chem. Soc. Rev.* **2010**, *39*, 2643.
- [3] J. Y. Kim, K. Lee, N. E. Coates, D. Moses, T. Q. Nguyen, M. Dante, A. J. Heeger, *Science* **2007**, *317*, 222.
- [4] H. K. Song, G. T. R. Palmore, *Adv. Mater.* **2006**, *18*, 1764.
- [5] Q. Wu, Y. Xu, Z. Yao, A. Liu, G. Shi, *ACS Nano* **2010**, *4*, 1963.
- [6] H. C. Lee, W. W. Liu, S. P. Chai, A. R. Mohamed, A. Aziz, C. S. Khe, N. M. S. Hidayah, U. Hashim, *RSC Adv.* **2017**, *7*, 15644.
- [7] Y. Wang, H. D. Tran, L. Liao, X. Duan, R. B. Kaner, *J. Am. Chem. Soc.* **2010**, *132*, 10365.
- [8] C. G. Wu, T. Bein, *Science* **1994**, *264*, 1757.
- [9] C. R. Martin, *Acc. Chem. Res.* **1995**, *28*, 61.
- [10] J. Ryu, C. B. Park, *Angew. Chem., Int. Ed.* **2009**, *48*, 4820.
- [11] L. Zhang, M. Wan, *Adv. Funct. Mater.* **2003**, *13*, 815.
- [12] H. Gao, T. Jiang, B. Han, Y. Wang, J. Du, Z. Liu, J. Zhang, *Polymer* **2004**, *45*, 3017.
- [13] G. M. Neelgund, A. Oki, *Polym. Int.* **2011**, *60*, 1291.
- [14] K. Su, N. Nuraje, L. Zhang, I. W. Chu, R. M. Peetz, H. Matsui, N. L. Yang, *Adv. Mater.* **2007**, *19*, 669.
- [15] N. Nuraje, K. Su, N. I. Yang, H. Matsui, *ACS Nano* **2008**, *2*, 502.
- [16] W. Chen, R. B. Rakhi, H. N. Alshareef, *J. Mater. Chem. A* **2013**, *1*, 3315.
- [17] Y. Long, Z. Chen, N. Wang, Y. Ma, Z. Zhang, L. Zhang, M. Wan, *Appl. Phys. Lett.* **2003**, *83*, 1863.

- [18] H. Ding, J. Shen, M. Wan, Z. Chen, *Macromol. Chem. Phys.* **2008**, 209, 864.
- [19] X. S. Du, C. F. Zhou, Y. W. Mai, *J. Phys. Chem. C* **2008**, 112, 19836.
- [20] X. Zhang, W. J. Goux, S. K. Manohar, *J. Am. Chem. Soc.* **2004**, 126, 4502.
- [21] J. Huang, R. B. Kaner, *Angew. Chem.* **2004**, 116, 5941.
- [22] J. Huang, R. B. Kaner, *J. Am. Chem. Soc.* **2004**, 126, 851.
- [23] J. Huang, S. Virji, B. H. Weiller, R. B. Kaner, *J. Am. Chem. Soc.* **2003**, 125, 314.
- [24] H. Qiu, J. Zhai, S. Li, L. Jiang, M. Wan, *Adv. Funct. Mater.* **2003**, 13, 925.
- [25] L. Wang, Y. Ye, X. Lu, Z. Wen, Z. Li, H. Hou, Y. Song, *Sci. Rep.* **2013**, 3, 3568.
- [26] K. Wang, Q. Meng, Y. Zhang, Z. Wei, M. Miao, *Adv. Mater.* **2013**, 25, 1494.
- [27] X. Zhou, T. Wu, B. Hu, G. Yang, B. Han, *Chem. Commun.* **2010**, 46, 3663.
- [28] Y. Zhang, X. Zhuang, Y. Su, F. Zhang, X. Feng, *J. Mater. Chem. A* **2014**, 2, 7742.
- [29] Y. Zhu, H. He, M. Wan, L. Jiang, *Macromol. Rapid Commun.* **2008**, 29, 1705.
- [30] S. Jafarzadeh, P. M. Claesson, P. E. Sundell, J. Pan, E. Thormann, *ACS Appl. Mater. Interfaces* **2014**, 6, 19168.
- [31] S. Li, D. Wu, C. Cheng, J. Wang, F. Zhang, Y. Su, X. Feng, *Angew. Chemie., Int. Ed.* **2013**, 52, 12105.
- [32] Y. Yan, J. Fang, Y. Zhang, H. Fan, Z. Wei, *Macromol. Rapid Commun.* **2011**, 32, 1640.
- [33] Z. Wei, T. Laitinen, B. Smarsly, O. Ikkala, C. F. J. Faul, *Angew. Chem., Int. Ed.* **2005**, 44, 751.
- [34] I. Y. Choi, J. Lee, H. Ahn, J. Lee, H. C. Choi, M. J. Park, *Angew. Chem., Int. Ed.* **2015**, 54, 10497.
- [35] B. Wang, L. Lucia, R.-D. Yang, K.-F. Chen, D.-T. Liu, W.-H. Gao, *J. Biobased Mater. Bioenergy* **2011**, 5, 197.
- [36] F. Song, J. Xu, W. G. Hou, *Chin. Chem. Lett.* **2010**, 21, 880.
- [37] B. Sun, J. Chai, Z. Chai, X. Zhang, X. Cui, J. Lu, *J. Colloid Interface Sci.* **2018**, 526, 9.
- [38] R. Sripriya, K. Muthu Raja, G. Santhosh, M. Chandrasekaran, M. Noel, *J. Colloid Interface Sci.* **2007**, 314, 712.
- [39] R. C. Foitzik, A. Kaynak, F. M. Pfeffer, *Tetrahedron* **2007**, 63, 4237.
- [40] I. Rodríguez, B. R. Scharifker, J. Mostany, *J. Electroanal. Chem.* **2000**, 491, 117.
- [41] B. Kong, A. Zhu, C. Ding, X. Zhao, B. Li, Y. Tian, *Adv. Mater.* **2012**, 24, 5844.
- [42] S. Li, W. Su, H. Wu, T. Yuan, C. Yuan, J. Liu, G. Deng, X. Gao, Z. Chen, Y. Bao, F. Yuan, S. Zhou, H. Tan, Y. Li, X. Li, L. Fan, J. Zhu, A. T. Chen, F. Liu, Y. Zhou, M. Li, X. Zhai, J. Zhou, *Nat. Biomed. Eng.* **2020**, 4, 704.
- [43] Y. Liu, H. Gou, X. Huang, G. Zhang, K. Xi, X. Jia, *Nanoscale* **2020**, 12, 1589.
- [44] C. L. Shen, Q. Lou, C. F. Lv, J. H. Zang, S. N. Qu, L. Dong, C. X. Shan, *Adv. Sci.* **2019**, 6, 1802331.
- [45] J. Xu, Y. Miao, J. Zheng, Y. Yang, X. Liu, *Adv. Opt. Mater.* **2018**, 6, 1800181.
- [46] V. Gupta, N. Chaudhary, R. Srivastava, G. D. Sharma, R. Bhardwaj, S. Chand, *J. Am. Chem. Soc.* **2011**, 133, 9960.
- [47] S. Zhu, Q. Meng, L. Wang, J. Zhang, Y. Song, H. Jin, K. Zhang, H. Sun, H. Wang, B. Yang, *Angew. Chem., Int. Ed.* **2013**, 52, 3953.